**Structural Engineering and Mechanics**, *Vol. 63, No. 3 (2017) 293-302*
DOI: https://doi.org/10.12989/sem.2017.63.3.293


# Investigation of load transfer along interfaces of jacketed square columns

Dimitra V. Achillopoulou*

*Department of Structural and Geotechnical Engineering, La Sapienza University of Rome, via Eudossiana 18, 00184, Italy*

*(Received November 2, 2016, Revised March 22, 2017, Accepted March 20, 2017)*

**Abstract.** This study deals with a numerical investigation of load transfer along interfaces of jacketed columns using finite element models. Appropriate plasticity and constitutive models are used to simulate the response of concrete and steel bars. Experimental data were used to calibrate the simulation of mechanical characteristics. The different compressive strength of core and jacket concrete, the confinement ratio, the dowels' diameter size and the load pattern shapes were considered. The path diagrams along the interfaces elucidate the areas around the dowel bars where due to stress concentration plastic hinges and intense discontinuities are created. The stress flow also depicts the contribution of confinement of the jacketed area to the overall resonant load capacity of the core column. The scope of the research is to identify and quantify the shear transfer along the interfaces of strengthened elements.

**Keywords:** RC jacketing; finite element model; interface; reinforced concrete; confinement

## 1. Introduction

Jacketing has been used as a rehabilitation method for many years. Various materials such as reinforced concrete jacketing, FRP's or steel plates have been used (Sengottaiyan and Jagadeesan 2013, Lei *et al*. 2012), resulting in different properties and capacity levels of the upgraded element. In all cases, the interface behavior is a crucial matter of design. All these methods have been proven to be efficient in enhancing the load capacity and the ductility of the retrofitted element. The strengthening design is found to be dependent on the interface capacity in transferring loads (Julio and Branco 2008, Achillopoulou *et al*. 2012, Achillopoulou and Karabinis 2013, Achillopoulou *et al*. 2013a, Achillopoulou *et al*. 2013b).

Numerical analysis was conducted in order to investigate the reliability of existing models to the prediction of the response of the rehabilitated element through RC jacketing. What is more, the finite element model permits a close micro-investigation in areas of high importance. In this way, results that are harder to obtain experimentally are thoroughly investigated.

In the present paper, an analytical investigation of the results of the interface of retrofitted concrete columns with RC jackets through a finite element model is presented. Appropriate plasticity and constitutive models are used to simulate the response of both concrete and rebars. A Drucker – Prager type model with an advanced approach in estimating plasticity parameters is inserted in FE code. All columns were retrofitted with RC jackets with various confinement ratios and dowel bars crossing the interface. All analytical results were compared and calibrated to previous research Achillopoulou *et al*. 2014, Alejano & Robert 2012). Though, this comparison is considered to be beyond the scope of the presented study. However, it was essential to calibrate mechanical properties of the used materials.

The main scope of the paper is mainly focused on the study of the response of the interface in an RC element jacketed with four-sided RC jacket. The findings of the research presented, help to better understand the overloaded areas of interest and the mechanism that contribute to it.

## 2. Specimens' characteristics and load patterns' shapes

Two different load pattern shapes were chosen:

• Load Pattern A (LPA) which provides full support of the jacket area and directly loads of the core's cross section in order to permit the core concrete to slide (Fig. 1(a)). This pattern was selected for the comprehension of the shear transfer mechanisms and its components along interfaces.

• Load Pattern B (LPB) describes the direct loading of core with the entire retrofitted element supported (Fig. 1(b)). That case simulates the function of a retrofitted column of a real structure where the axial load flows through the old column (core). Even if the jacket crosses the beam- column joint, the jacket's concrete presents shrinkage phenomena, due to the different time of casting. As a result a region of the old column is not fully jacketed.

The investigation includes nine specimens. Three are imposed to LPA and the rest to LPB. Two columns were made of plain concrete (24 MPa core concrete, 31 MPa jacket concrete) loaded either in LPA or in LPB. Five specimens contained dowel bars of 10mm diameter ($f_y$=566 MPa), three of them with core and jacket confinement ($\omega_{cc}$=0.15, $\omega_{cj}$=0.035/0.075/0.142, $f_y$=250 MPa).

Finally, two specimens contained only dowel bars of 14

*Corresponding author, Ph.D.
E-mail: Dimitra.achillopoulou@uniroma1.it


http://www.techno-press.com/journals/sem&subpage=7
ISSN: 1225-4568 (Print), 1598-6217 (Online)

Table 1 Specimens' reinforcement details

| No | Specimens | $b_c \cdot h_c$ (mm·mm) | $b_{(j+c)} \cdot h_{(j+c)}$ (mm·mm) | $\rho_{lc}$ (%) | $D_{bwc}$ (mm) | $s_{wc}$ (mm) | $\omega_{wc}$ | $D_{bwj}$ (mm) | $s_{wj}$ (mm) | $\omega_{wj}$ | $D_b$ (mm) | $\rho_{db}$ | Interface Definition |
|---|---|---|---|---|---|---|---|---|---|---|---|---|---|
| 1 | A-S-UR | 150·150 | 310·310 | 1 | - | - | - | - | - | - | - | - | S |
| 2 | A-S-URDb=14 mm | 150·150 | 310·310 | 1 | - | - | - | - | - | - | 14 | 0,0021 | Teflon |
| 3 | A-S-URDb=10 mm | 150·150 | 310·310 | 1 | - | - | - | - | - | - | 10 | 0,0016 | Teflon |
| 4 | B-S-UR | 150·150 | 310·310 | 1 | - | - | - | - | - | - | - | - | S |
| 5 | B-S-URDb=14 mm | 150·150 | 310·310 | 1 | - | - | - | - | - | - | 14 | 0,0021 | Teflon |
| 6 | B-S-URDb=10 mm | 150·150 | 310·310 | 1 | - | - | - | - | - | - | 10 | 0,0016 | Teflon |
| 7 | B-S-RcRjDb-1 | 150·150 | 310·310 | 1 | 5,5 | 50 | 0,15 | 5,5 | 100 | 0,035 | 10 | 0,0016 | S |
| 8 | B-S-RcRjDb-2 | 150·150 | 310·310 | 1 | 5,5 | 50 | 0,15 | 5,5 | 50 | 0,071 | 10 | 0,0016 | S |
| 9 | B-S-RcRjDb-3 | 150·150 | 310·310 | 1 | 5,5 | 50 | 0,15 | 5,5 | 25 | 0,142 | 10 | 0,0016 | S |
| 10 | B-R-RcRjDb-1 | 150·150 | 310·310 | 1 | 5,5 | 50 | 0,15 | 5,5 | 100 | 0,035 | 10 | 0,0016 | R |
| 11 | B-R-RcRjDb-2 | 150·150 | 310·310 | 1 | 5,5 | 50 | 0,15 | 5,5 | 50 | 0,071 | 10 | 0,0016 | R |
| 12 | B-R-RcRjDb-3 | 150·150 | 310·310 | 1 | 5,5 | 50 | 0,15 | 5,5 | 25 | 0,142 | 10 | 0,0016 | R |

Notes:

| | | | |
|---|---|---|---|
| $b_c$: core's cross section width | A: Load pattern | $D_{bwc}$: Bar diameter of core stirrup | $\omega_{wj}$: Jacket's mechanical percentage |
| $h_c$: core's cross section height | S: Smooth interface | $D_{bwj}$: Bar diameter of jacket stirrup | $D_b$: Dowels bar diameter |
| $b_{(j+c)}$ : core's & jacket's cross section width | UR: Unreinforced concrete | $S_{wc}$: Core's stirrups spacing | $\rho_{db}$: Volumetric % of interface reinforcement |
| $h_{(j+c)}$ : core's & jacket's cross section height | $R_c$: Reinforced core | $S_{wj}$: Jacket's stirrups spacing | |
| $\rho_{lc}$: percentage of longitudinal reinforcement of core | $R_j$: Reinforced jacket | $\omega_{wc}$: Core's mechanical percentage | |

mm ($f_y$=566 MPa). The interface of two specimens was covered with polymeric sheets in order to limit friction effect. All specimens' characteristics and dimensions are shown in Table 1 and Figure 1. The percentage and spacing of dowels placed at the interface are attuned according to EN 1998-3.

## 3. Finite element analysis using advanced plasticity model

Finite element analysis enables the nonlinearities of the simulated materials and the contact surfaces, meaning the interfaces of the used elements. Suitable discretization helps the macro or micro investigation of several structural unsolved or undefined problems. In this way, reliable FE analysis requires consideration of suitable models for materials and their interactions (Karabinis *et al*. 2008, Kwan and Ng 2013, Jiang and Wu 2012). The models for concrete and steel inserted in Abaqus finite element software are presented as follows.

Concrete is modelled as a Drucker-Prager type material exploiting findings derived from experimental investigation of plastic parameters. The Drucker-Prager model was chosen due to its simplicity, its smooth and symmetric failure surface in the stress- space which makes less trivial its incorporation in softwares. Differently from other simulation models (Concrete Damage Plasticity, Smear Cracking etc) the Drucker-Prager model takes into consideration triaxial stresses (principal $\sigma_1', \sigma_2', \sigma_3'$) with the same weight. As a result in some cases stresses are overestimated (Alejano and Bobet 2012). Concrete is modelled using a solid eight-node element. A Drucker-Prager failure criterion was adopted in the form given by Eq. (1)

$$F=\sqrt{(J_{2D})}\ F(K)+\theta I_1-K=0 \tag{1}$$

where $J_{2D}$ is the second invariant of stress deviator, $J_1$ is the first invariant of stress and $\theta$ is the friction parameter. Function $f(K)$ is an indirect expression of Lode's angle combining third and second invariant of deviatoric stress. It accounts for the variation of shear strength of concrete for different load paths and a given hydrostatic pressure and determines the shape of failure function in deviatoric plane. The shape of deviatoric plane changes from a circle to a curved triangle for different values of material parameter $K$. Hardening-softening parameter $K$ is derived by Eq. (2)

$$K=[(1/\sqrt{3}-\theta)]\ \sigma_c \tag{2}$$

where $\sigma_c$ is the unconfined concrete strength. Analysis incorporates stress-plastic strain behavior of plain concrete according to indirect estimation so as to take into account hardening-softening behavior of concrete. A Drucker-Prager type plastic potential function $G$ is used according to Eq. (3)

$$G=\sqrt{(J_{2D})}\ f(K)+f(a)J_1 \tag{3}$$

where $f(\alpha)$ is an expression of the parameter of plastic dilatation of concrete that affects the direction of plastic strain vector. A non-associated flow rule is considered, meaning that the direction of plastic strain vector is normal to a limit surface (plastic potential surface G, Jankowiak and Łodygowski 2015) that differs from the failure surface F.

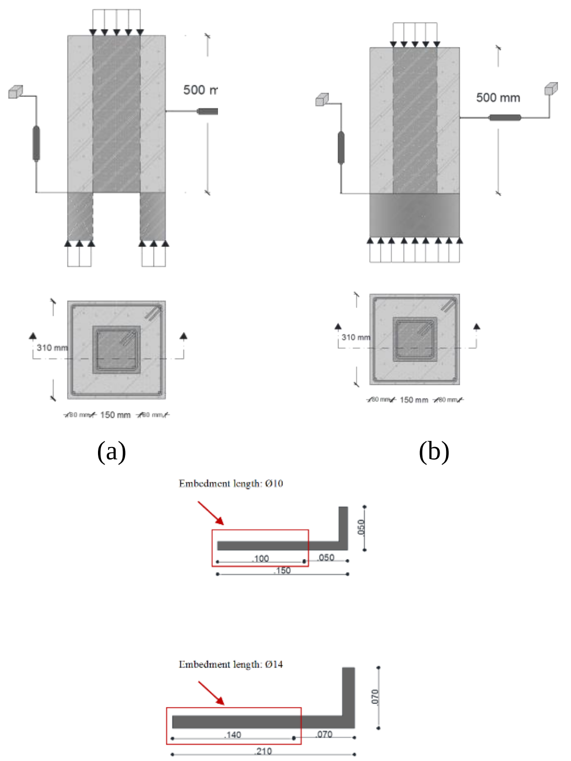

(c)

Fig. 1 Load pattern shapes: (a) Load Pattern A (LPA), (b) Load Pattern B (LPB), (c) embedment length of dowel bars

As previous researchers have already stated (Arslan 2007) the dilation and friction affect the analysis results since the constitutive law changes. Interface properties affect also the analytical data. The determination of maximum shear stress and cohesion parameters were essential in order to achieve an agreement with experimental results. In fact, the values of each parameter were chosen after brazilian tests of concrete (for tensile stress, $f_t$=2.62 MPa) and the cohesion and friction values from the (pull-off) test of the unreinforced sample (A-S-UR, $c$=0.73 MPa, $\varphi$=21.4°).

The contact model used is a linear elastic plane four-node element (node to surface contact) using penalty parameters and Langrange multipliers which practically includes all degrees of freedom of the contact. Through this parameters are attributed all the equivalents and failure models that could have a frictious spring in the contact.

Steel reinforcement is modelled using a solid eight-node element considering a material that yields and hardens (longitudinal bars, stirrups, dowels). In case of premature buckling (elastic or plastic) of steel rebars under compression, the stress-strain response is modified according to relations. Traditionally steel rebars are simulated using a bar element embedded to the concrete masses with attributed steel performance. This work tries to naturally represent the steel bars and the fractures evolving around them.

The Finite Element Analysis included the following steps:

• Determination of the geometry of the simulated model.

• Definition of the material and contact properties.

According to previous studies conducted at the same concrete regimes the dilatancy and friction parameters are: angle of friction equals to 48, flow stress ratio equals to 1 and dilation angle equals to 50. Literature includes an oversupply of research in this field, the review of which exceeds the limits of this work.

• Section and contact assignment.

Solids were modelled with a 8node solid element and interfaces were modelled using 6 nodes or 8nodes interface elements taking into consideration delamination law depending on the connection (surface to surface or point to surface). It is attributed the Mohr- Coulomb isotropic friction criterion for the interface response. The friction coefficient and the maximum shear stress as well as the elastic coefficient was defined according to Eq. (4)

$$\tau = k_s \cdot \gamma^{el} \quad (4)$$

where: $k_s$: interface stiffness

Friction between the different parts is attributed using a stick and a slip bond law through a maximum tangential force. In this way, the relative displacement of the interface is calculated in every load step and possible gaps formed are well described. The different kind of interfaces are simulated by different values of tangential force (the rough interface exhibits higher friction coefficient and as such the corresponding force).

• Discretization of the model as well as the density of discretization is determined depending on the number of seeds in each surface and the suitable meshing technique. The main target of meshing is the simplicity and compatibility of nodes' positions among elements in contact so as to avoid convergence problems. Mesh size was governed by the smallest region created while forming the parts of the specimen. In this way the nodes of the different parts coincide. Moreover, the imposed displacement of each step is chosen to be smaller or equal to the finite elements' size, in order not to be comparable larger. The mesh refinement if not proper enables convergence problems (if nodes of different parts do not coincide) or results in large displacements.

• Monotonic axial displacement is imposed on the core's concrete section according to the load pattern presented in the shape of Fig. 1(a).

• Determination of the boundary conditions. In the case of reinforced concrete columns, where ¼ of the section is modelled (because of symmetry in loading and geometry of the specimen), the specimen has to be constrained suitably in symmetry planes. Matrices are solved according to Eq. (5)

$$[K] \cdot \{u\} = \{F^a\} \quad (5)$$

Where:

$[K]$: is the stiffness matrix

$\{u\}$: is the vector of the numbers of DOF values

$\{F^a\}$: is the vector of imposed displacements

Analysis includes non-linearities simulating concrete fractures. The equilibrium of steps is accomplished by a time-step analysis where the final force vector is reached imposing the load in steps and following Newton-Raphson

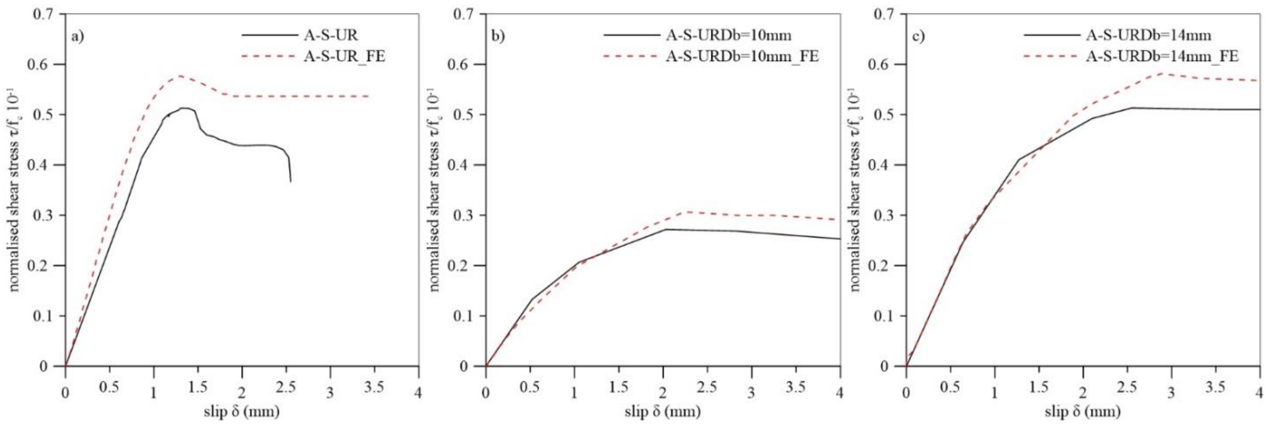


Fig. 2 Normalized shear stress ($\tau/f_c$·10-1) versus slip cures (δ) of smooth interface- LPA

convergence method (Eq. (6))

$$[K_{(n,1)}{}^{T}]\cdot\{\Delta_{ui}\}=\{[F_n]^a\}-\{F_{(n,1)}{}^{nr}\} \quad (6)$$

Where:
$K_{n,1}{}^{T}$: is the tangent matrix for time step $n$, iteration $i$
$F_n{}^{a}$: is the total applied force vector at time step $n$
$F_{n,1}{}^{nr}$: is the is the restoring force vector for time step $n$, iteration $i$

## 4. Validation of experimental and numerical results

Fig. 3 shows the comparative diagram of experimental and analytical results for the normalized shear stress ($\tau/f_c$) versus slip ($s$). It is generally noted that the experimental results presented in this work is a part of a wider experimental program conducted for a wider research. As such here is presented a set of samples for each category and the mean curve and in no case an independent specimen. It presents analytical and experimental results of specimens with smooth interfaces subjected to load pattern A (LPA). Analytical results of the unreinforced specimen (Fig. 2(a)) present negligible differences (5%) of shear stress levels comparing with the corresponding experimental ones. The noticeable loss of stress at slip value of 1.25mm is due to the absence of cohesion of old and new concrete and appears in lower values (16%) in respect to the experiments. Since differences are of no significant importance, the assumption of the applied models and constitutive laws are confirmed and are proven to predict sufficiently the percentage of cohesion loss and its corresponding slip, overestimating though stress (in tolerable limits to consider accurate).

Fig. 2(b) presents the shear stress of an unreinforced element with concrete connectors (dowel bars) of 10mm diameter and no friction at the interface of both concretes. The differences in this case are focused more on the maximum stress of the analytical results which is 7% higher than tests. Finally, Fig. 2(c), presents the case of an unreinforced specimen with concrete connectors of 14 mm diameter with almost zero friction. Analytical stress results are 10% augmented in relation to the experimental ones. For both connectors diameter size, the initial stiffness coincides with the one measured in tests.

One can comment on the differences observed and analyzed in this part (experiments, finite element model). Though, it is considered that the differences are negligible regarding the phenomena that need to be illuminated. In fact, the slip values between the interfaces are of a very small magnitude. In real structures or different load patterns and load diffusion, slip values are even smaller. If one examines the values of slip that each international standard takes into account, the simulation is satisfactory, safe and represents reality.

In addition, the test conducted was better used to assess and confirm the values of the interface parameters included in codes, taking into account the four sided jacket effect. Slant shear tests lack of this phenomenon. In all cases, values are at the same regime and magnitude.

## 5. Finite element analysis results and discussion

The presented Figures include the results of specimens that are simulated through Finite Element Models, 11 in number. Table 1 includes specimens' characteristics. Figures show diagrams of normal stresses as a ratio of the maximum stress of the element ($\sigma_{33}/\sigma_{33\max}$) at the edge of the interface of core and jacket versus the normalized height of the specimen ($h_1/h_{tot}$). Additionally, flow stress diagrams along the connectors length (dowel bars) are presented as a function of the normalized length ($l_1/l_{tot}$).

Figs. 3, 4 show the analytical results of force transferring between core and jack*et al*ong the interface (LPA). Fig. 3(c), (d) and Fig. 4(c), (d) show the stress allocation on the interface of an element with concrete connectors (dowels). The unreinforced specimen of LPA, having smooth interface, presents an appreciable decrease of carrying load, almost in a fixed rate. Due to symmetry and the absence of reinforcement, the same behavior is noted at the perpendicular side. Unlikely, the jacket presents continuous increase of stress along the interface (Fig. 4(a)). The levels of undertaken stress of both core and jacket in every position of the interface illustrates the progressive force transfer from core to jacket through aggregate interlock and cohesion. The pattern of Fig. 5 shows that crack growing is diffusing from the diagonal direction of the core's cross section, forming cracks parallel to the

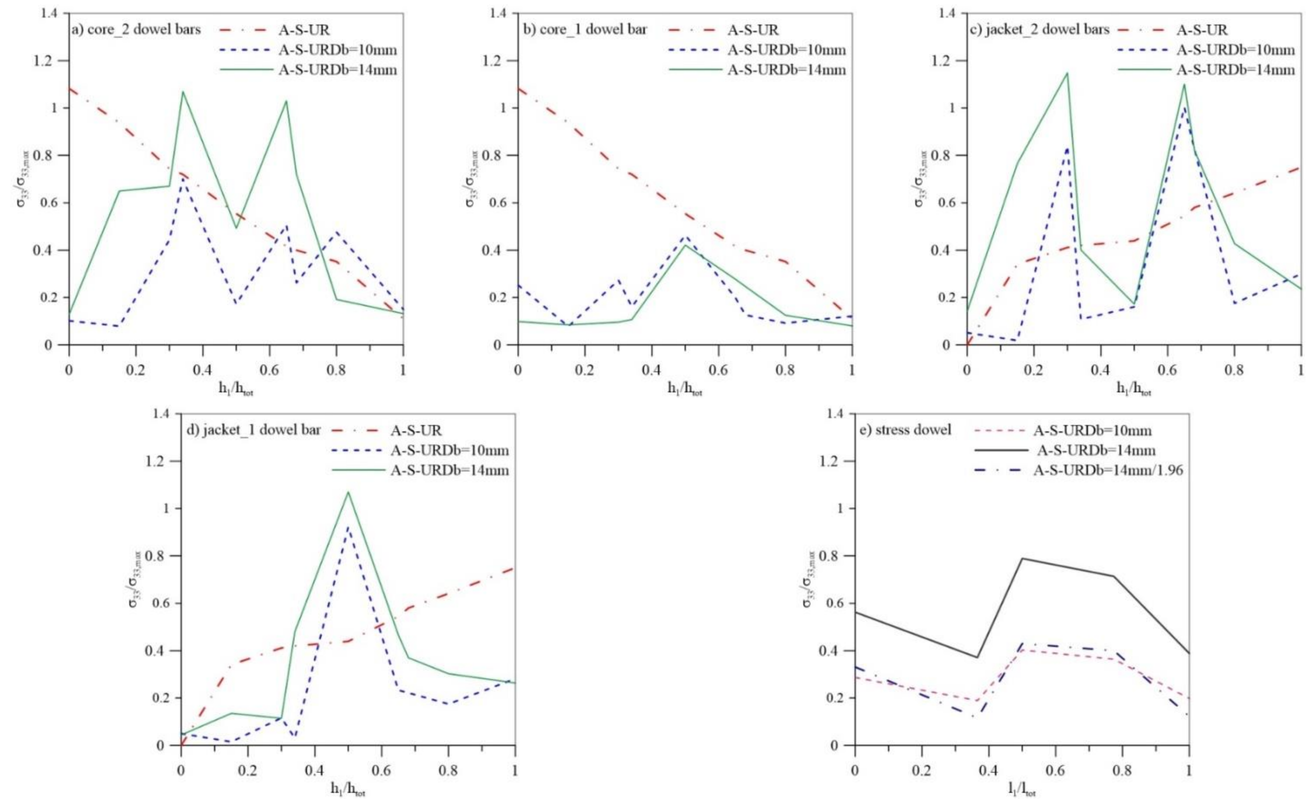


Fig. 3 Stress allocation results of FEA of smooth interface- LPA

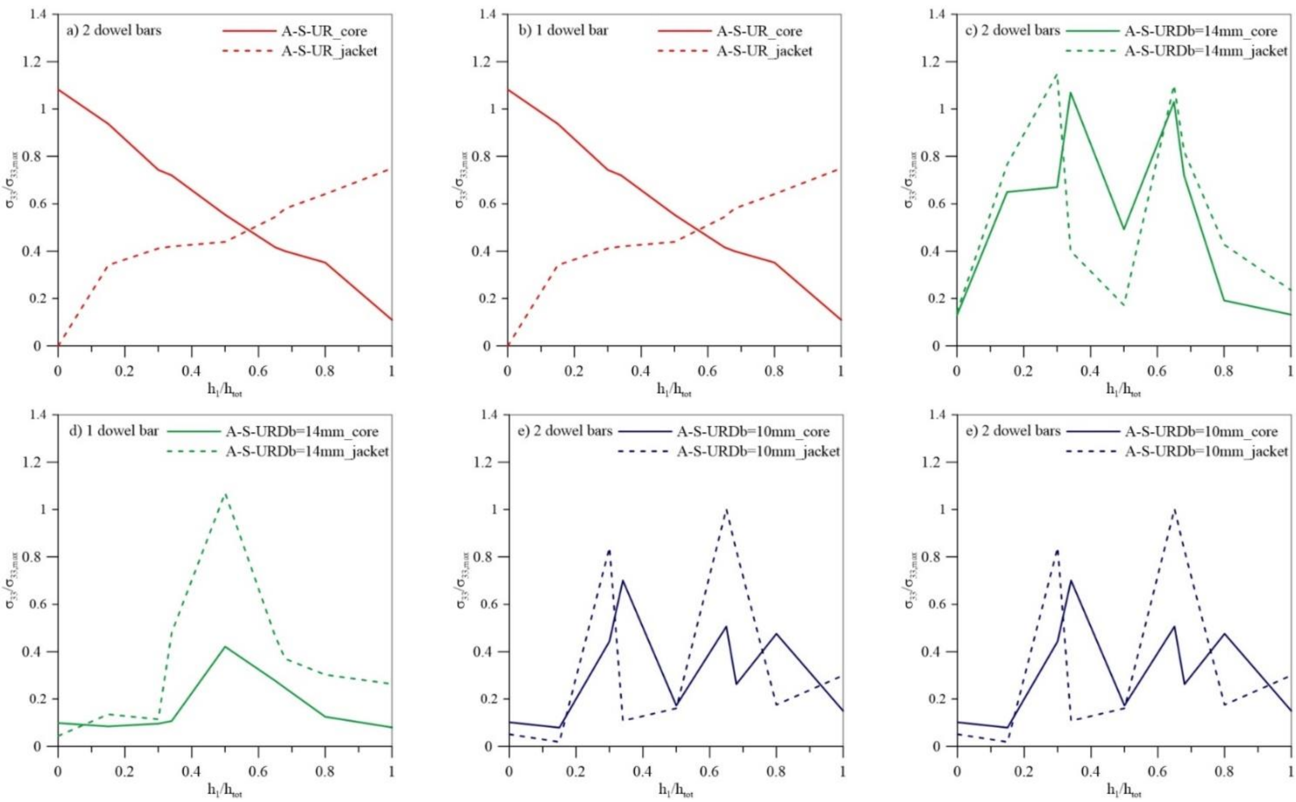


Fig. 4 Force transfer of smooth interface-LPA

interface length both in core and jacket. Failure was formed in the same way experimentally (Fig. 6). Due to the core's slip, the ultimate position is located in the level higher than the interface length in which stresses are zero.

Specimens containing concrete connectors (dowels) present local stress fluctuation. More specifically, at the two

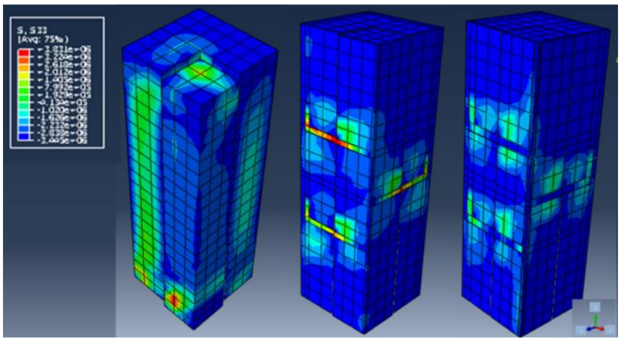

Fig. 5 Finite element analysis' results- crack pattern plots

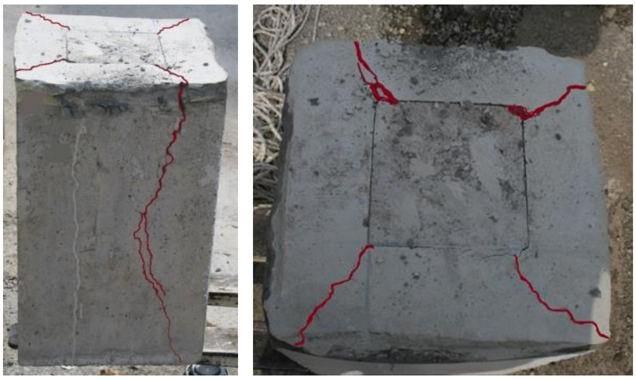

Fig. 6 Crack patterns of unreinforced specimen with smooth interface- LPA

consecutive sides different number of connectors are placed and as a result stress interruption is presented at the connectors' positions. Specimen A-S-URDb=14 mm presents reduction of core stress along the interface in both sides (Fig. 3(c),(d)). In fact, due to the lack of friction between the two concretes, stress in both sides is gathered around and transferred through the connectors. Similar behavior is presented in the presence of connectors of 10 mm diameter.

The differentiation in respect to the specimen containing larger diameter connectors is located to the percentage of the stress concentration around the dowel bars. The difference of stress is higher in the first dowel position, at the other positions the reduction ranges to 14%. Figure 3e shows the stress allocation along the connectors' length both for 10 and 14mm. It is noted that in the interface point ($l_1/l_{tot}$=0.5), the stress level is the highest. In fact after the interface point, stress is reduced due to the force transferring from core to jacket through dowels.

If the stress of the largest diameter dowel bar is normalized to the ratio of dowels' area ($\pi d^2_{14}/4$ / $\pi d^2_{10}/4$= 1.96) allocation coincides. As a conclusion the carrying stress is proportional to the bar's area and dowels' action remains shear. The simulation proves analytically and comes in agreement with past research on dowel action (Achilllopoulou D.V. 2016).

Fig. 4 presents a comparison between core's and jacket's stress of LPA along the interface of both sides. In every position the abstraction between core's and jacket's stress represents the transferred load from old to new element.

Diagram of Fig. 7 shows the analytical results of specimens for LPB. It includes results of an unreinforced specimen (B-S-UR) and two specimens containing concrete connectors of 10 and 14 mm diameter with zero friction (ideally smooth interface).

It is noted that core's stress in all specimens is augmented and higher compared to the jacket's corresponding stress. The jacket itself acts as an additional confinement mean with favorable effect on the element's load capacity. In cases that friction is absent and connectors are placed, there is a remarkable stress concentration at the dowel positions in both sides. In this case core undertakes higher stress. In fact, by raising the connector's diameter,

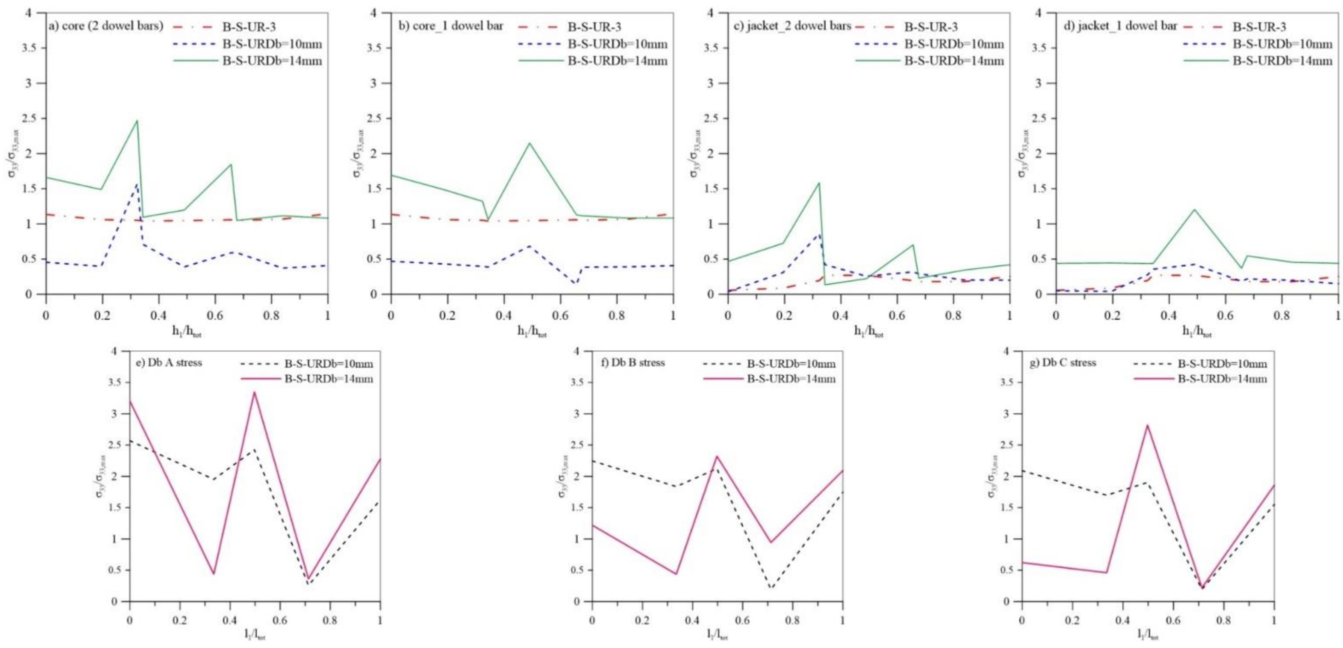


Fig. 7 Stress allocation results of FEA of smooth interface- LPB

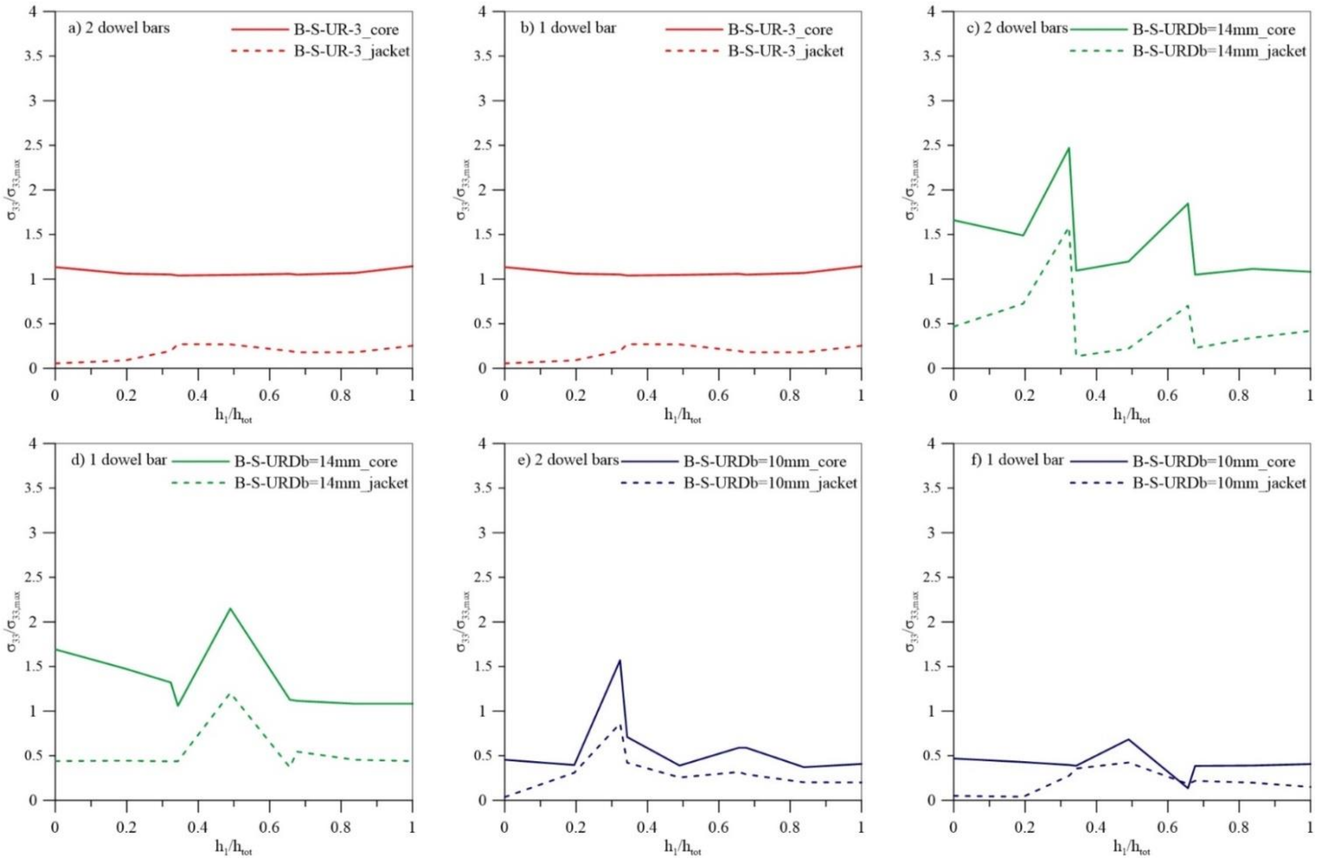


Fig. 8 Force transfer of smooth interface- LPB

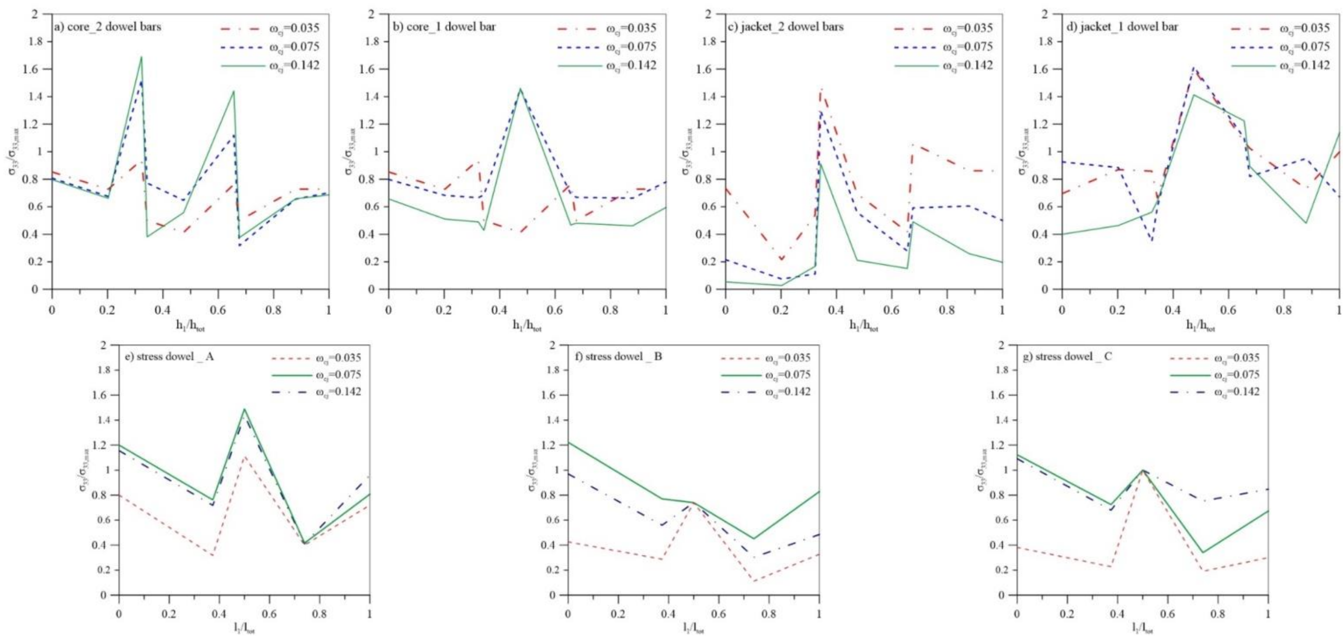


Fig. 9 Stress allocation of confined specimens containing dowel bars- smooth interface- LPB

core concrete carries 60% higher load compared to the B-S-URDb=10 mm specimen at the side with two bars (Fig. 7(a), (c)) and up to 3 times higher at the side with one bar (Fig. 7(b), (d)). Finally, the allocation and distribution to the different connectors is shown to Fig. 7(e), (f), (g). Dowel bar A, placed at the 1/3 of the specimen's height, is stressed more in relation to the others (B, D) for both different diameters. The maximum stress is appointed at the connectors' middle point. From this point and on, the whole load is transferred to the jacket. Fig. 9 presents the load transfer in this case. It is worth noticing that due to the load pattern shape (LPB) core has a quasi-stable level of

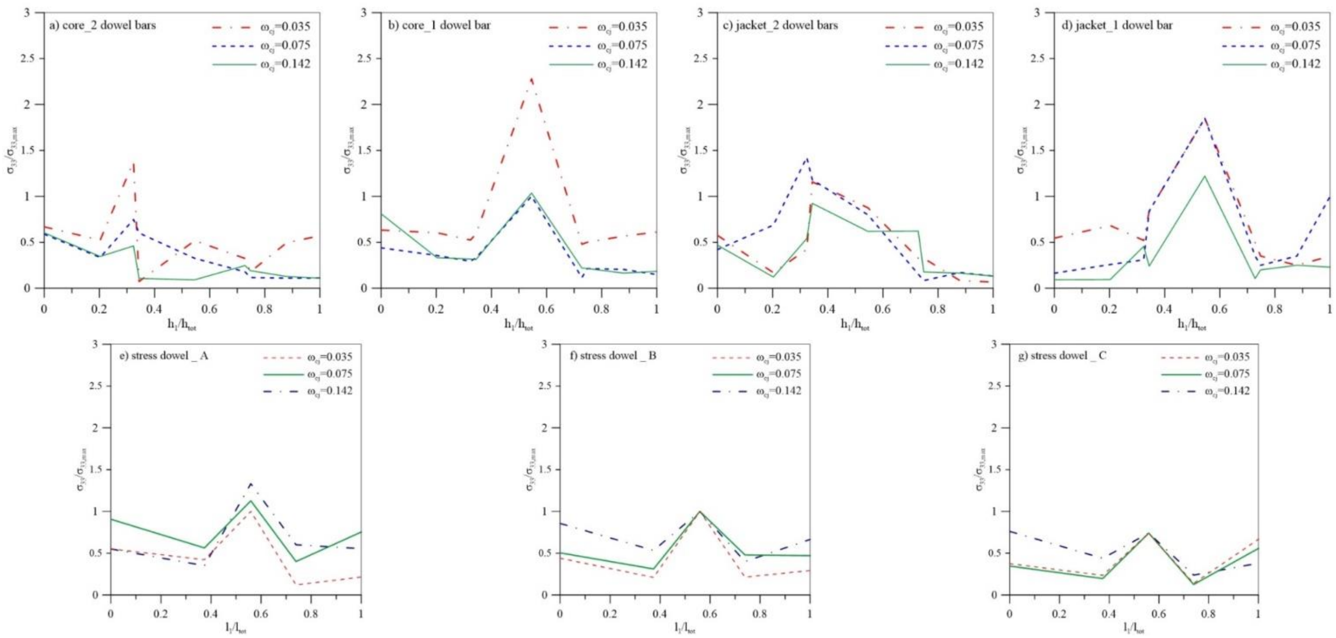


Fig. 10 Stress allocation of confined specimens containing dowel bars- rough interface- LPB

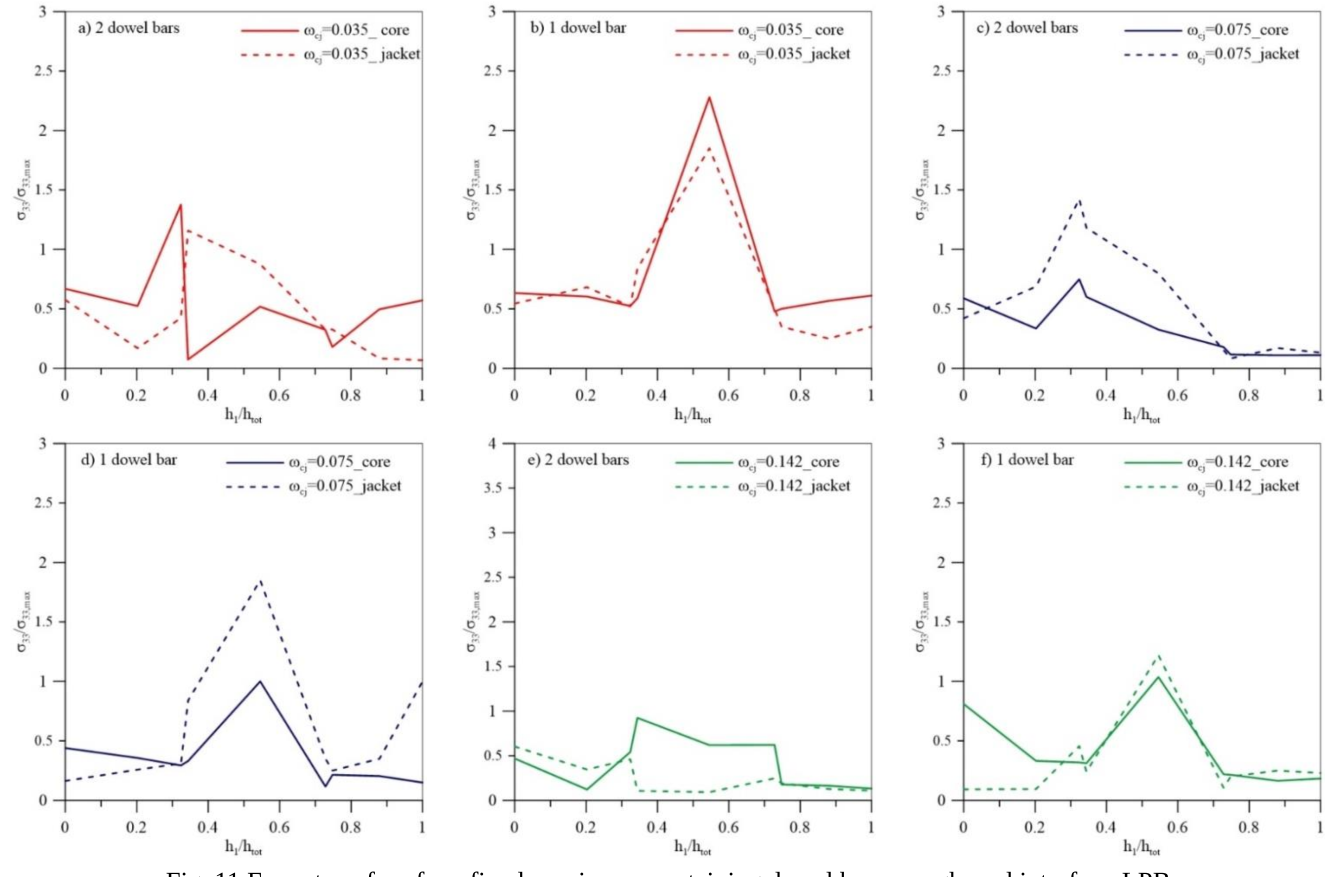


Fig. 11 Force transfer of confined specimens containing dowel bars- roughened interface-LPB

carrying load, especially in the absence of connectors (Fig. 8(a), (b)). In the presence of dowel bars (Fig. 8(c), (d), (e), (f)) specimens present similar behavior as in load pattern A (LPA). For the shake of brevity the percentages are not discussed in the current part. Fig. 10(c) presents the stress allocation along the smooth interfaces of confined specimens with concrete connectors (dowels) of 10 mm diameter for Load Pattern B. By raising confinement, core's stress rises at the side where two connectors are placed (Fig. 9(a), (c)). At the face where only one connector is placed (Fig. 9(b), (d)), the maximum stress ranges at the same percentages for all confinement levels of the jacket. Closer stirrup spacing of the jacketed area leads to higher normal stress provided to the interface which acts favorably to the core's load capacity. The three connectors depending on the position in which they are placed are differently stressed. At the first level, for the case of the highest jacket's confinement ratio, jacket's stress is lower than core's (Fig. 11(b)). At the second level ($h_1/h_{tot}$=0.5), the maximum load of the dowel bar is presented at the core's side.

At the lowest level, stress at the interface position is 25% higher compared to the corresponding stress of dowel at level B. Stress concentration at the core's concrete and at the connectors' positions and levels is an overloading hint to detect local damages. These fractures are created for strains surpassing the limits of elastic design, therefor damages are permanent, plastic hinges and discontinuities are created due to the crack width.

Fig. 10 shows the stress allocation along the roughened interfaces of specimens of Load Pattern B with concrete connectors of 10 mm diameter for three confinement ratios. In order to simulate roughness a proper friction coefficient was used and calibrated as the other parameters of the tests. It is of high importance to point out that stress is concentrated at the first connector bar (dowel A) for both jacket (Fig. 10(c), (d)) and core (Fig. 10(a), (b)). At the second connector bar (dowel B), that is the side where only one dowel is placed, stress ratios are higher for low jacket's confinement ratio.

As observed in the cases of smooth interfaces, high jacket's confinement leads to higher stress levels of core's concrete. What is more, dowels present a gradual reduction of stress depending on the level they are placed. Differences in jacket's confinement ratio lead to negligible range of the first connectors' stress (Figure 10a). At the interface point for upper and lower dowel level and all stirrup ratio, the stress is practically the same (Figure 10b,c). Figure 11 shows the transferred load from core to jack*et al*ong the interface path. It is noted, that by augmenting jacket's confinement the percentage of the transferred load is diminished. In this way it is confirmed that the jacket acts as an additional passive confinement, raising core's load capacity.

## 6. Conclusions

The development of finite element models has contributed to the directions of detailed simulations. The interface comprehension is an unsolved issue which can be better explained and accomplished if proper models were used, attributing contact and mechanical properties. Apart from the contour plots, path diagrams are a useful tool to investigate and quantify the load transfer ratios along the interface and the overloaded areas. Due to stress concentration around the dowel bars intense discontinuities are noted. Concrete presents a non-linear response and plastic hinges are created resulting to open cracks. The crack patterns show that the weakest concrete of the interface (core's concrete) is disorganized the most. Examining further the dowel action in isolation from other shear mechanisms, it is concluded that the friction absence helps to understand better the capacity of connectors and the plastic hinges around the dowels. It is proven that dowels act in shear, in all slip values, and that the load capacity is an area dependent and not diameter dependent propety.

The interface treatment changes behavior. Smooth interfaces containing dowels, if compared to roughened ones, exhibit higher load capacity. The aggregate interlock action is dominant and diffuses stresses to the jacket's concrete, relieving dowel bars from load. In cases of roughened interfaces, the first connector is imposed to higher stress rate. Regardless the confinement ratio, no differences are noted in terms of dowels' maximum stress. On the whole, elements present up to 43% higher stress. The jacket's confinement, though, is a factor contributing favorably to the core's capacity load.

## References

Achilllopoulou, D.V. (2016), "Understanding the basic mechanisms acting on interfaces: concrete elements, materials and techniques", *Adv. Mater. Interf.*, 205-247.

Achillopoulou, D.V. and Karabinis, A.I. (2013), "Investigation of shear transfer mechanisms in repaired damaged concrete columns strengthened with RC jackets", *Struct. Eng. Mech.*, **47**(4), 575-598.

Achillopoulou, D.V., Pardalakis, T. and Karabinis, A.I. (2014), "Construction deficiencies effect on the behavior of reinforced concrete columns under repeated axial loads_experimental and analytical investigation", Transactions of the VŠB-Technical University of Ostrava, **14**(2), Civil Engineering Series.

Achillopoulou, D.V., Pardalakis, T.A. and Karabinis, A.I. (2013), "Investigation of force transfer mechanisms in retrofitted RC columns with RC jackets containing welded bars subjected to axial compression", *ECCOMAS Thematic Conference-COMPDYN 2013: 4th International Conference on Computational Methods in Structural Dynamics and Earthquake Engineering, Proceedings-An IACM Special Interest Conference*, 4029-4038.

Achillopoulou, D.V., Skeparnis, E. and Karabinis, A.I. (2014), "Investigation of the interface behaviour of retrofitted concrete columns through finite element analysis", *Second European Conference on Earthquake Engineering and Seismology*, Instabul.

Achillopoulou, D.V., Tasiopoulos, T.P.K. and Karabinis, A.I. (2013), "Study of the behavior of RC columns strengthened with RC jackets containing dowels and different confinement ratios", *Thematic Conference-COMPDYN 2013: 4th International Conference on Computational Methods in Structural Dynamics and Earthquake Engineering, Proceedings - An IACM Special Interest Conference*, 4018-4028.

Alejano, L.R. and Bobet, A. (2012), "Drucker-Prager criterion", *Rock Mech. Rock Eng.*, **45**(6), 995-999.

Arslan, G. (2007), "Sensitivity study of the Drucker-Prager modeling parameters in the prediction of the nonlinear response of reinforced concrete structures", *Mater. Des.*, **28**(10), 2596-2603.

EN 1998-3 (2005), Eurocode 8: Design of structures for earthquake resistance-Part 3: Assessment and retrofitting of Buildings.

He, X.G. and Kwan, A.K.H., (2001), "Modelling dowel action of reinforcement bars for finite element analysis of concrete structures", *Comput. Struct.*, **79**(6), 595-604.

Jankowiak, T. and Łodygowski, T. (2015), *Plasticity Conditions* *and Failure Criteria for Quasi-brittle Materials*, Handbook of Damage Mechanics Nano to Macro Scale for Materials and Structures.

Jiang, J.F. and Wu, Y.F. (2012), "Identification of material parameters for Drucker-Prager plasticity model for FRP confined circular concrete columns", *Int. J. Solid. Struct.*, **49**(3-4), 445-456.

Julio, E.N.B.S. and Branco, F.A.B. (2008), "Reinforced concrete jacketing- interface influence on cyclic loading response", *ACI Struct. J.*, **105**(4), 471-477.

Karabinis, A., Rousakis, T. and Manolitsi, G. (2008), "3D finite-element analysis of substandard RC columns strengthened by fiber-reinforced polymer sheets", *J. Compos. Construct.*, **12**(5), 531-540.

Kwan, A.K.H. and Ng, P.L. (2013), "Modelling dowel action of discrete reinforcing bars for finite element analysis of concrete structures", *Comput. Concrete*, **12**(1), 19-36.

Lei, D., Chen, G., Chen, Y. and Ren, Q. (2012), "Experimental research and numerical simulation of RC beams strengthened with bonded steel plates", *Science China Technological Sciences*, 1-8.

Sengottaiyan, K. and Jagadeesan, K., (2013), "Retrofitting of columns with RC jacketing an experimental behavior", *J. Theor. Appl. Inform. Technol.*, **56**(3), 349-354

Teng, J.G. and Lam, L. (2004), "Behavior and modeling of fiber reinforced polymer-confined concrete", *J. Struct. Eng.*, ASCE, **130**(11), 1713-1723.

*CC*